Petroleum 5 (2019) 171–177

Contents lists available at ScienceDirect

Petroleum

journal homepage: www.keaipublishing.com/en/journals/petlm

A slug capturing method in unconventional scenarios: The 5ESCARGOTS code applied to non-Newtonian fluids, high viscous oils and complex geometries

Marco Ferrari [a], Arianna Bonzanini [b], Pietro Poesio [b, *]

[a] Department of Mathematics, Politecnico di Milano, P.zza Leonardo Da Vinci 32, 20133 Milan, Italy
[b] Department of Mechanical and Industrial Engineering, Università degli Studi di Brescia, via Branze 38, 25123 Brescia, Italy

ARTICLE INFO

Article history:
Received 16 August 2017
Received in revised form
12 October 2017
Accepted 31 January 2018

ABSTRACT

Previous work showed that a one-dimensional, hyperbolic, transient five-equation two-fluid model can predict automatically the formation, growth, and subsequent development of slugs in horizontal and near-horizontal flow. This method was implemented in a finite volume numerical scheme – called 5ESCARGOTS code. Comparison with experimental data showed that it can be used to predict the flow pattern and statistical characteristics (slug velocity, length, and frequency). However, the capabilities of this approach have been tested only for water-air flows in a straight horizontal pipe.

In this work, we validate the application of the code to some unconventional problems. Firstly, we test the possibility of slug capturing approach to describe and predict the relevant features of air/high viscosity oils or air/non-Newtonian fluids flows. Comparisons between some slug characteristics and empirical correlations, available in literature, are discussed. Then, we move from simple geometries toward more complex conditions that may be representative of actual application cases, also employing high viscous oils as liquid phase. Comparison against experimental data shows results in reasonable agreement.

1. Introduction

Slug flow is a typical flow regime that occurs in many engineering scenarios, such as in oil and gas industry, chemical process, and energy production systems. In horizontal and near horizontal pipes, this flow pattern arises from stratified flow due to the growth of small perturbations, which may appear at the interface between liquid and gas and then may grow into larger waves until they fill completely the pipe. Moreover, slug flow can also occur at changes in pipe slope, for example when the pipe inclination, initially horizontal or downward, turns upward generating a v-section: here the liquid accumulates because of gravity. As consequence, the liquid volume fraction increases until the stratified-slug flow transition occurs.

Often, slug flow characteristics are numerically computed by steady-state method, such as the *unit-cell* approach, see Refs. [1–3], or by transient models, as in the *empirical slug specification* method – [4–6] – and in *slug tracking*, see Refs. [7,8]. However, as pointed out by Issa and Kempf [9], these method have some limits: in particular, they are not able to predict automatically the transition between flow patterns.

Among transient models, Issa and Kempf [9] introduced a third method, called *slug capturing*, where stratified, slug, and transition regimes are described by the same set of equations and closure relations. The slug development, i.e. formation, growth, and decay, is naturally described by the numerical solution of the transient two-fluid model, written for stratified flow. When the liquid volume fraction increases and tends to unity, slug formation is an automatic outcome of the numerical computation. In other words, slug flow is established in a natural manner from the computed

* Corresponding author.
E-mail addresses: marco2.ferrari@polimi.it (M. Ferrari), a.bonzanini001@unibs.it (A. Bonzanini), pietro.poesio@unibs.it (P. Poesio).

Peer review under responsibility of Southwest Petroleum University.

Production and Hosting by Elsevier on behalf of KeAi

https://doi.org/10.1016/j.petlm.2018.01.005

flow because of hydrodynamic instabilities emerging from stratified flow – for details see Ref. [9]. Applications and improvements of this method can be found also in Refs. [10–12].

However, the four-equation two-fluid model adopted in these works to describe the stratified flow, is affected by ill-posedness, as noticed also by Issa and Kempf [9]. The ill-posedness of the two-fluid model is a critical issue, as pointed out by many Authors, see Refs. [13,14]. Well-posedness is strictly linked to hyperbolicity – [15,16] – and, therefore, some methods that make the two-fluid model hyperbolic have been developed during the last decades, see Ref. [15] for an overview of these methods. Among these methods, the mathematical regularization technique introduced by Baer and Nunziato [17] and by Saurel and Abgrall [18] consists in the addition of a transport equation for the gas volume fraction to the four-equation two-fluid model: it has been demonstrated that the addition of this equation enforces hyperbolicity and closes the system. This five-equation two-fluid model has been adopted by other few Authors, see Refs. [19,20].

Recently, Ferrari et al. [21] developed a numerical scheme that solves a hyperbolic five-equation two-fluid model with compressible phases. They show the capability of their code to predict slug flow characteristics by a slug capturing method. Their system is closed by a pressure relaxation process and pressure terms are written in a consistent way to represent a two-phase stratified flow, as prescribed by Brauner and Moalem Maron [22]. The five-equation model adopted and modified by Ferrari et al. [21] for slug capturing purpose has three main advantages, compared to other two-fluid models available in literature:

(1) It is hyperbolic, without the addition of a viscous term;
(2) It accounts for the physical effect of surface tension avoiding the numerical issues due to the introduction of a second order derivative in the computation of the curvature function; this derivative is solved separately from the main model, within the pressure relaxation process;
(3) The hypothesis of long waves, which is usually adopted by other Authors to disregard the viscous term (losing, meantime, the hyperbolicity and the physical effect that this term describes), is here not necessary.

The numerical algorithm developed in Ref. [21] is based on the high-resolution finite volume scheme, called *Roe*5, previously presented by Munkejord [23]. Ferrari et al. [21] modified the *Roe*5 scheme to account for their closure models and they added a numerical criterion to capture automatically flow regime transitions, avoiding the singularities which characterize a two-fluid model when the liquid volume fraction tends to unity. They showed that their code is grid independent, and able to capture transitions between stratified, wavy, and slug flow adopting very low thresholds in the transition criterion, if compared to the codes developed by other Authors. Finally, they computed the main slug characteristics and flow pattern map for air-water flow in horizontal pipe: presented results are in good agreement with empirical correlations or experimental data available in literature.

This paper presents a direct extension to some unconventional scenarios of the previous work by Ferrari et al. [21]: the same mathematical model and numerical method are here adopted to demonstrate that the code implemented in Ref. [21] is applicable and able to simulate slug conditions in two-phase flows where the liquid phase is a high-viscous oil or a non-Newtonian fluid, or where the pipe configuration is characterized by a more complex geometry than a horizontal one.

The paper is organized as follows: Sections 2 and 3 briefly recall the five-equation two-fluid model and the numerical method previously presented by Ferrari et al. [21], respectively. In Section 4, the results of simulations applied to some unconventional scenarios, such as air/high-viscous oil, air/non-Newtonian fluid, and complex geometries, compared to empirical correlations or experimental data, are presented. Finally, conclusions are discussed in Section 5.

2. Model

To describe a two-phase flow, the five-equation, hyperbolic, one-dimensional, two-fluid model widely investigated by Ferrari et al. [21] is adopted. Under the assumption of isothermal flow, i.e. the energy equations are neglected, the model consists in five time-dependent partial differential equations, where four of them are derived from the conservation of mass and momentum for each phase. A fifth equation, which expresses the evolution of the gas volume fraction, is added to the system. The system is written as

$$\frac{\partial \alpha_g}{\partial t} + u_i \frac{\partial \alpha_g}{\partial x} = r_p\left(p_{ig} - p_{il}\right), \tag{1}$$

$$\frac{\partial\left(\alpha_g \rho_g\right)}{\partial t} + \frac{\partial\left(\alpha_g \rho_g u_g\right)}{\partial x} = 0, \tag{2}$$

$$\frac{\partial(\alpha_l \rho_l)}{\partial t} + \frac{\partial(\alpha_l \rho_l u_l)}{\partial x} = 0, \tag{3}$$

$$\begin{aligned}&\frac{\partial\left(\alpha_g \rho_g u_g\right)}{\partial t} + \frac{\partial\left(\alpha_g \rho_g u_g^2\right)}{\partial x} + \alpha_g \frac{\partial p_{ig}}{\partial x} + \rho_g \alpha_g g \frac{\partial h}{\partial x}\cos(\vartheta)\\ &= -\rho_g \alpha_g g \sin(\vartheta) - F_{gw} - F_i,\end{aligned} \tag{4}$$

$$\begin{aligned}&\frac{\partial(\alpha_l \rho_l u_l)}{\partial t} + \frac{\partial\left(\alpha_l \rho_l u_l^2\right)}{\partial x} + \alpha_l \frac{\partial p_{il}}{\partial x} + \rho_l \alpha_l g \frac{\partial h}{\partial x}\cos(\vartheta)\\ &= -\rho_l \alpha_l g \sin(\vartheta) - F_{lw} + F_i,\end{aligned} \tag{5}$$

where the subscripts l and g stand for liquid and gas phase, respectively; the subscript i indicates the interfacial variables and the subscript w specifies the wall. α is the volume fraction, ρ is density and u stands for phase velocity; p is the pressure, p_{ig} and p_{il} indicate gas and liquid interfacial pressures, respectively. As indicated in Fig. 1, θ is the inclination angle, and g stands for the gravity acceleration. The frictional forces per unit volume are represented by the F terms: they call for closure relations, which are explained in Section 2.2. The variable h is the height of the liquid surface, as shown in Fig. 1. The pressure formulation in momentum Eqs. (4)–(5) derives from the average pressure value at each phase in stratified conditions, as prescribed by Brauner et al. [22]. Finally, the equations are complemented by the relation between the volume fractions of the two phases,$\alpha_g + \alpha_l = 1$.

Thanks to the addition of Eq. (1) to the four-equation two-fluid model, the five-equation system becomes hyperbolic. Obviously, Eq. (1) needs a closure relation for the interfacial velocity u_i: Saurel and Abgrall [18] estimate it as

$$u_i = \frac{\sum \alpha_k \rho_k u_k}{\sum \alpha_k \rho_k}, \tag{6}$$

which represents the velocity of the centre of mass. The subscript k stands for the generic phase.

In the Eq. (1), r_p represents the pressure relaxation parameter. In this paper, pressure relaxation is solved by an instantaneous pressure relaxation process, as proposed by Saurel and Abgrall [18] and further discussed in Refs. [21,23]. As shown by Ferrari et al. [21], the

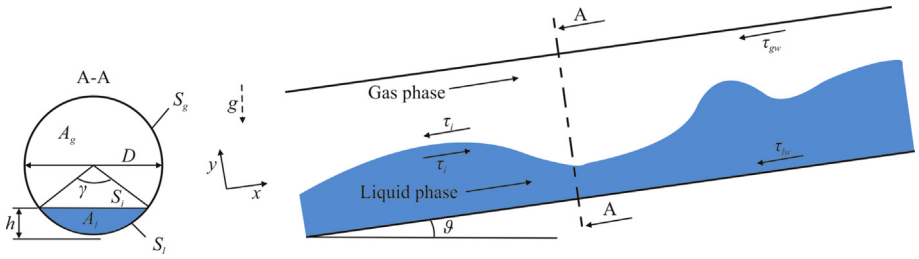

Fig. 1. Geometry.

pressure relaxation process allows to account for surface tension effects without the issues due to the difficulties which often characterize the numerical solution of this term, when inserted by other Authors into their two-fluid model to ensure the hyperbolicity (here provided, instead, by the addition of Eq. (1) to the system). Moreover, as already observed in Section 1, this fact allows to avoid the hypothesis of long waves, usually introduced in other works to disregard the second order derivative that appears in the viscous term formulation. However, Ferrari et al. [21] showed that surface tension has a negligible effect on a liquid-air two-phase flow in horizontal pipe; then, in the present paper, the possibility to account for this effect is disregarded.

As proved by many Authors [21,23], the five-equation system (1)–(5), with instantaneous pressure relaxation, provides a strictly hyperbolic alternative to the traditional four-equation two-fluid model. Moreover, this model is suitable for slug capturing, as shown and discussed by Ferrari et al. [21]. Thanks to all these peculiar characteristics, we chose to adopt this model in this work.

2.1. Equation of state (EOS)

In the five-equation model, liquid and gas phases are both assumed to be compressible, hence the balance Eqs. (1)–(5) must be closed with the equation of state

$$p_k = c_k^2\left(\rho_k - \rho_{k,0}\right) - p_0, \tag{7}$$

which relates densities to pressures; c_k is the speed of sound in phase k, $\rho_{k,0}$ and p_0 are the reference values for density and pressure, respectively.

2.2. Closure models

The liquid-wallF_{lw}, gas-wallF_{gw} and interfacial F_i shear forces calls for closure relations. In this paper, they are defined as

$$F_{lw} = \frac{\tau_{lw}S_l}{A},\quad F_{gw} = \frac{\tau_{gw}S_g}{A},\quad F_i = \frac{\tau_i S_i}{A}, \tag{8}$$

where, as shown in Fig. 1, A is the cross-section area, S_l, S_g are the perimeters wetted by the liquid and gas phases, respectively, and S_i stands for the cross section of the interfacial surface between the two phases.

Shear stresses τ are written as

$$\tau_{lw} = \frac{1}{2}f_{lw}\rho_l|u_l|u_l,\quad \tau_{gw} = \frac{1}{2}f_{gw}\rho_g|u_g|u_g,$$

$$\tau_i = \frac{1}{2}f_i\rho_g|u_g - u_l|(u_g - u_l). \tag{9}$$

Here, we adopt the same friction factors formulation prescribed in previous works about slug capturing, see Refs. [21,9].

The gas-wall friction factors and the interfacial friction factor correlations adopted in case of turbulent flow are

$$f_g = \begin{cases} \dfrac{16}{Re_g} & \text{if } Re_g < 2100 \\ 0.046(Re_g)^{-0.2} & \text{if } Re_g \geq 2100 \end{cases}, \tag{10}$$

$$f_i = \begin{cases} \dfrac{16}{Re_i} & \text{if } Re_i < 2100 \\ 0.046(Re_i)^{-0.2} & \text{if } Re_i \geq 2100 \end{cases}. \tag{11}$$

Whereas, for liquid-wall friction friction factor we use

$$f_l = \begin{cases} \dfrac{24}{Re_l} & \text{if } Re_l < 2100 \\ 0.0262(\alpha_l Re_{sl})^{-0.139} & \text{if } Re_l > 2100 \end{cases}. \tag{12}$$

Finally, the Reynolds numbers are defined as follows

$$Re_g = \frac{4A_g u_g \rho_g}{(S_g + S_i)\mu_g}, Re_i = \frac{4A_g|u_g - u_l|\rho_g}{(S_g + S_i)\mu_g},$$
$$Re_l = \frac{4A_l u_l \rho_l}{(S_l)\mu_l}, Re_l = \frac{Du_{sl}\rho_l}{\mu_g}. \tag{13}$$

Referring to Fig. 1, the parameters in Eq. (13) are defined as: D is the pipe internal diameter, A_g and A_l represents the pipe cross section occupied by the gas and liquid phase, respectively; μ stands for the dynamic viscosity and u_{sl} indicates the liquid superficial velocity.

3. Numerical method

As done in some other works, see Refs. [21,23], the system of Eqs. (1)–(5) is discretised on a uniform one-dimensional grid, by a finite volume method and by a first order explicit discretisation in time. The numerical solution is here obtained through a succession of operators in a fractional-step process

$$\boldsymbol{Q}_i^{n+1} = \boldsymbol{L}_s^{\Delta t}\boldsymbol{L}_h^{\Delta t}\boldsymbol{Q}_i^n, \tag{14}$$

where $\boldsymbol{Q}_i^n$ is the numerical approximation of the vector of variables in the cell i and at time n, whereas $\boldsymbol{Q}_i^{n+1}$ is the same vector at time $n + 1$. Then, the solution is updated at each iteration through two sequential sub-steps.

1. In the first sub-step, in each cell i, to solve the hyperbolic system

$$\frac{\partial \boldsymbol{q}}{\partial t} + \boldsymbol{A}(\boldsymbol{q})\frac{\partial \boldsymbol{q}}{\partial x} = 0, \tag{15}$$

which contains non-conservative terms, we apply the

hyperbolic operator $\boldsymbol{L}_h^{\Delta t}$.

This step calls for the solution of the linear Riemann problem at cells interface. To do that, a Roe method is adopted. This leads to an upwind resolution of the wave phenomena appearing in the problem and the solution of the Riemann problem is obtained basing on the *Roe*5 solver by Munkejord and Gran [23]. This solver computes, at each iteration, the value of the unknown vector $\boldsymbol{Q}_i^{h,n+1}$ by a high resolution extension of Godunov's method. The high resolution correction guarantees a second order accuracy in space.

2. Then, in a second sub-step, the addition of source terms appearing in momentum Eqs. (4)–(5) is applied by the operator $\boldsymbol{L}_s^{\Delta t}$. Moreover, this operator takes into account the pressure relaxation process as well, where, if necessary, the surface tension effect is accounted for. For details, see Ref. [21].

   Moreover, in Ferrari et al. [21] the *Roe*5 scheme is modified to account for the pressure terms in stratified flow conditions, to correctly model shear forces, and to describe the transition from two (i.e. stratified flow) to one phase (i.e. slug flow). Indeed, during the slug onset process, the transition from two-phase flow to single phase flow occurs, and the liquid volume fraction grows and tends to unity; conversely, the gas volume fraction tends to zero and this generates numerical problems as discussed by Munkejord and Gran [23]. Ferrari et al. [21] introduced a slug criterion to handle these numerical issues, allowing a correct slug capturing numerical simulation.

Ferrari et al. [21] implemented this numerical method in a code called **5ESCARGOTS**, which is adopted in this work.

4. Results

4.1. High viscous oils

According to Nicklin [24], the velocity of gas bubbles in the air/oil slug flow is well approximated by the relation

$$u_t = C_0 u_m + u_d, \tag{16}$$

where C_0 is the distribution parameter, u_m is the mixture velocity, u_d is the drift velocity. This equation is used to fit data from experiments in order to obtain a correlation for the slug translation velocity for air/oil flows.

We try to numerically simulate an air/high-viscous oils two-phase flow in a horizontal pipe and to compare computed slug velocities with empirical correlations available in literature. We focus especially on the trend of slug velocities as function of mixture velocities, checking if Eq. (16) is respected.

The pipe is horizontal ($\theta = 0°$) with length $L = 40.0\,m$ and internal diameter $D = 0.0508\,m$. Phase constants for EOS, Eq. (7), are reported in Table 1. Numerical simulations are performed with an oil with a viscosity of $\mu_l = 0.150\,Pa \cdot s$; air viscosity is taken equal to $\mu_g = 1.79 \cdot 10^{-5}\,Pa \cdot s$. The outlet is open to ambient pressure.

The numerical parameters are set constant for all simulations: the time step is $\Delta t = 1.0 \cdot 10^{-5}\,s$, while the cells number is equal to 1000 ($\Delta x/D = 0.79$) and the CFL = 0.25.

A first test setting superficial velocities as $u_{sg} = 1.0\,m/s$ and $u_{sl} = 1.0\,m/s$ is performed. Fig. 2 shows that the code predicts a reasonable slug flow formation in time along the pipe and it gives a qualitative idea of how slug flow develops.

Table 1
Constants for the EOS, Eq. (7), for air/oil flow.

	$c_k\,[m/s]$	$\rho_{k,0}\,[kg/m^3]$	$\mu_k\,[Pa \cdot s]$
air (g)	316	1.0	$1.79 \cdot 10^{-5}$
oil (l)	1000	850.0	0.150

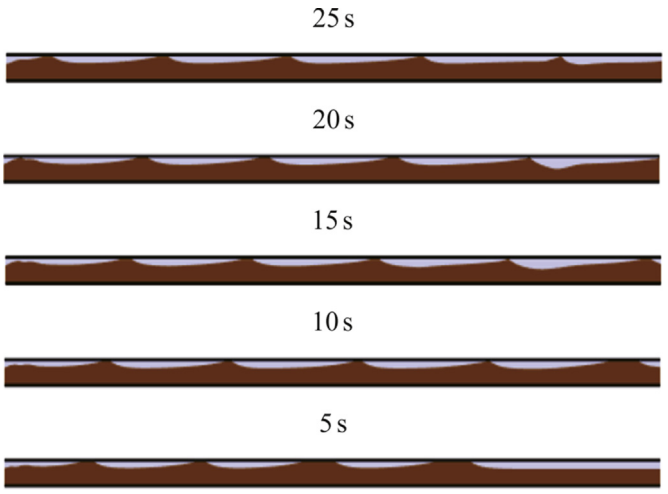

Fig. 2. Air/high viscous oil flow in horizontal pipe. Slug flow evolution. Oil coloured in brown.

Then, we simulate the same air/oil two-phase flow varying inlet superficial velocities: the oil and gas superficial velocities are chosen in the range $(0.8 \div 2.0)\,m/s$ and $(0.1 \div 6.0)\,m/s$, respectively.

In Fig. 3 numerically computed slug velocities, compared to an experimentally obtained relation – Foletti et al. [25] – are presented: numerical data are in quite good agreement with the trend predicted by experiments, with a maximum error of about 25%.

4.2. Non-Newtonian fluids

Two-phase gas/liquid flows where the fluid has a shear-thinning behaviour are often involved in chemical and oil industry processes. Only few experimental studies have been done regarding this particular type of two-phase flow. Picchi et al. [26] performed some experiments on gas/non-Newtonian fluid two-phase flow in horizontal and near horizontal pipes. In particular, they created experimental flow pattern maps comparing experimental observations to the theoretical stratified flow existence region.

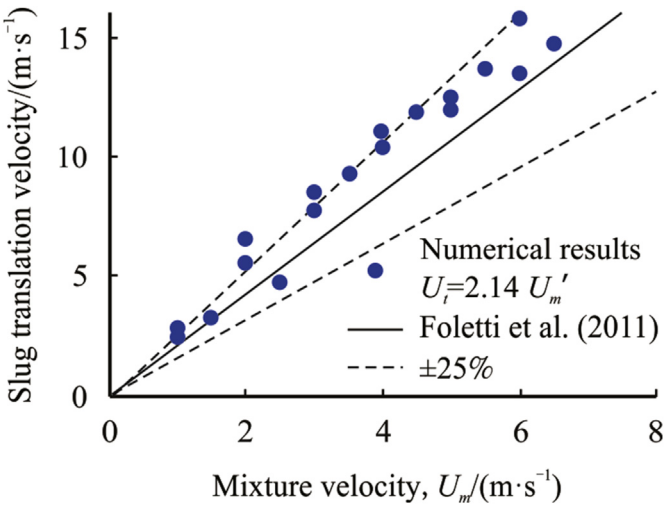

Fig. 3. Air/high viscous oil flow in horizontal pipe. Slug mean velocity as function of mixture velocity.

Table 2
Physical constants for CMC-6, comparison against water.

	Conc. [%]	c_k [m/s]	$\rho_{k,0}$ [kg/m^3]	m [$Pa \cdot s^n$]	n [-]
water (l)	–	1000	1000	0.001	1
CMC-6 (l)	6	1000	1002	0.264	0.757

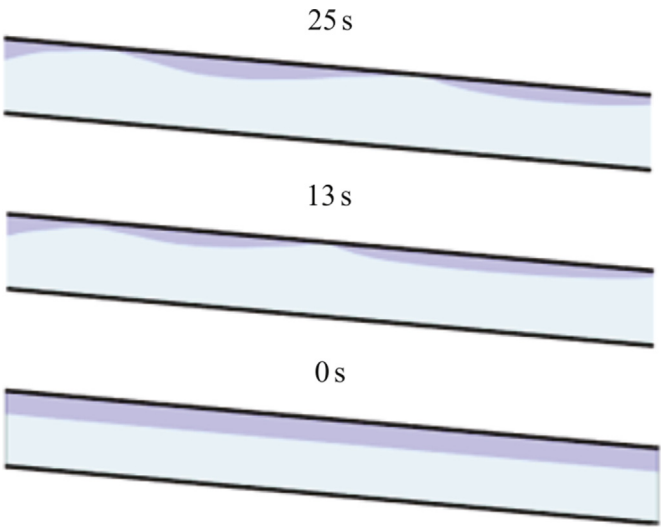

Fig. 4. Air/non-Newtonian fluid flow. Slug flow evolution. CMC-6 coloured in cyan.

Our purpose is the creation of a flow pattern map through numerical simulations to observe if our code is able to simulate gas/non-Newtonian fluid two-phase flows and to predict the correct transition between stratified and slug flow.

Assuming that fluid has a power-law rheological behaviour, Picchi et al. [26] consider the shear stress τ related to the shear rate $\dot{\gamma}$ by $\tau = m(\dot{\gamma})^n$, where m and n are two fitting parameters that represent the fluid consistency index and the flow behaviour index, respectively. Under this assumption, we have to take into account the different behaviour of a non-Newtonian fluid in the mathematical definition of closure relations for shear stress, see Section 2.2. In particular, we must change the formulation of the Reynolds number for the liquid phase Re_l from Eq. (13) to

$$Re_l = \left(\frac{4A_l}{S_l}\right)^n \frac{u_l^{2-n}\rho_l}{m8^{n-1}\left(\frac{1+3n}{4n}\right)^n}, \tag{17}$$

In their experiments, Picchi et al. [26] employed, as liquid phase, a shear-thinning fluid obtained by adding Carboxymethyl Cellulose (CMC) to water in concentration of 6%. The same experimental setup has been simulated by the 5ESCARGOTS code: an air/CMC-6 two-phase flow in a pipe 5° downward inclined, with diameter and length equal to 0.022 m and 9.0 m, respectively. Physical properties of CMC-6 are reported in Table 2 in comparison with water properties.

All simulations are performed with $\Delta t = 1.0 \cdot 10^{-5}\, s$, $\Delta x/D = 1.02$, and CFL = 0.44. In Fig. 4 the evolution of the liquid volume fraction is reported. Liquid and gas superficial velocities are set to 0.86 m/s and 0.61 m/s, respectively. The transition from stratified flow to slug flow is clearly visible.

In order to obtain a flow pattern map, 60 simulations are performed with different couples of superficial velocities: for gas phase, superficial velocities are set in the range (0.1 ÷ 2.0) m/s; instead, for non-Newtonian liquid phase, they are chosen between 0.05 m/s and 0.87 m/s.

Fig. 5a shows the experimental map obtained by Picchi et al. [27]; conversely, in Fig. 5b flow regimes obtained by numerical simulations are reported. The green line represents the *zero characteristics* (ZRC) boundary which gives the region of existence of the stratified flow regime computed by the two-fluid model predictions, see Ref. [12].

Comparing the two flow pattern maps of Fig. 5, we can observe that, since the gas entrainment is neglected in our model, see Section 2, we are not able to identify the differences between slug and plug flow; so we consider all flows that are not stratified as slug flow. Moreover, although numerical results are in good agreement with theoretical predictions (ZRC line), Fig. 5b shows that the transition between stratified and slug flow begins at values of liquid superficial velocity higher than the ones observed experimentally. This can be due to the numerical diffusion that affects the computational scheme, explained in Section 3, which tends to smooth little instabilities which can eventually develop into slugs. For details about this issue see Ref. [21].

4.3. TUFPP loop

In this Section, we present an example of a more complex configuration. It is an air-high viscous oil flow in a pipe characterized by a length of 41 m, an internal diameter $D = 0.0508\, m$, and composed by three different consecutive parts: as shown in Fig. 6, the first part is 20 m long with an upward inclination $\theta = 2°$, the second one, with a length $L = 1\, m$, is horizontal, and, finally, the last part is 20 m long and downward inclined, with $\theta = -2°$. This configuration is the reproduction of the TUFPP loop of the University of Tulsa (OK, US). Constant parameters that appear in EOS -

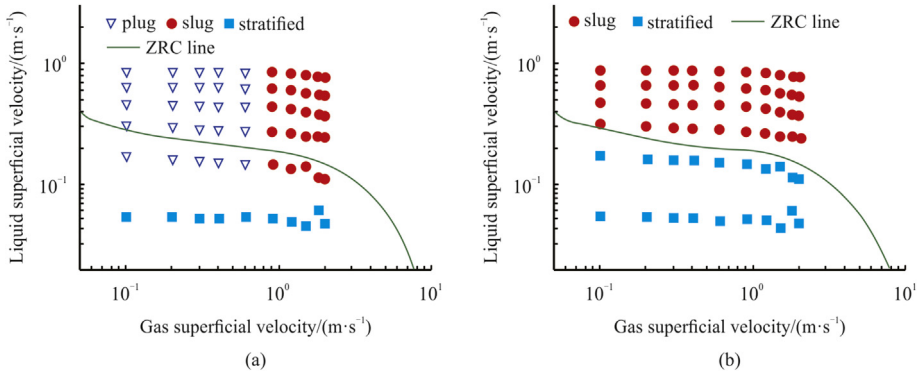

Fig. 5. Air/non-Newtonian fluid flow. Slug flow evolution. Comparison between experimental (a) – Picchi et al. [27] – and numerical (b) flow pattern map.

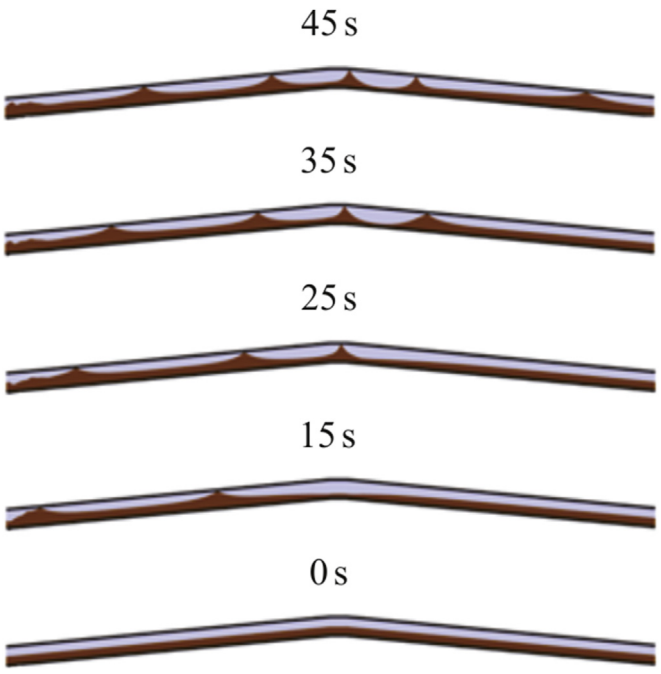

Fig. 6. TUFPP loop. Slug flow evolution. Oil coloured in brown.

Eq. (7) - are reported in Table 1. Viscosities are set to $\mu_g = 1.79 \cdot 10^{-5}\, Pa \cdot s$ for the gas phase, and to $\mu_l = 0.155\ \mathrm{Pa} \cdot s$ for the liquid one. Inlet gas and liquid superficial velocities are fixed equal to $u_{sg} = 0.6\, m/s$ and to $u_{sl} = 0.08\, m/s$, respectively, whereas the outlet is open to ambient.

Numerical parameters are set as follows: the time step is equal to $\Delta t = 1.0 \cdot 10^{-5}\, s$, while the cells number is 900 ($\Delta x/D = 0.9$) with a CFL of 0.22.

For this particular configuration, the theoretical model, as the one proposed by Brauner and Moalem Maron [28], predicts slug flow only in the first upward inclined part of the pipe, and stratified flow in the third downward inclined part. Some experiments carried out recently on the TUFPP loop have shown that the flow regime predicted by the theoretical model is in agreement with experimental observations in the first part of the pipe only (the upward inclined one): in fact, in the downward inclined branch, actual flow shows slug conditions. Fig. 6 shows results computed by the numerical code adopted in this work: the numerical simulation produces the same behaviour of experiments, and the slug flow appears in the last downward inclined part of the pipe as well.

5. Conclusions

In this paper numerical simulations of two-phase flow in some unconventional scenarios using a one-dimensional, hyperbolic, five-equation two-fluid model have been presented. This work represents an extension of the work previously presented by Ferrari et al. [21]. Some actual applications are simulated to evaluate the ability of the code to predict slug flow onset, evolution and characteristics in unconventional cases. The **5ESCARGOTS** code is able to simulate not only standard air-water flow situations, see Ref. [21], but also air-high viscous oil flow, air/non-Newtonian flow, and configuration characterized by more complex geometry. In all the cases analysed in this work, results are in good agreement with empirical correlations or experimental observations available in literature.

Since very few works about transient numerical simulations of slug flow in unconventional scenarios have been carried out previously by other Authors, the encouraging results presented here represent a first step to the application of academic numerical code to the simulation of more actual configurations, closer to industrial problems.

References

[1] A.E. Dukler, M.G. Hubbard, A model for gas-liquid slug flow in horizontal and near horizontal tubes, Ind. Eng. Chem. Fundam. 14 (1975) 337–347, https://doi.org/10.1021/i160056a011.
[2] Y. Taitel, D. Barnea, Two-phase slug flow, Adv. Heat Tran. 20 (1990) 83–132, https://doi.org/10.1016/S0065-2717(08)70026-1.
[3] G.B. Wallis, One-Dimensional Two-Phase Flow, McGraw-Hill, 1969.
[4] V. De Henau, G.D. Raithby, A transient two-fluid model for the simulation of slug flow in pipelines - I. Theory, Int. J. Multiphas. Flow 21 (1995) 335–349, https://doi.org/10.1016/0301-9322(94)00082-U.
[5] V. De Henau, G.D. Raithby, A transient two-fluid model for the simulation of slug flow in pipelines - II. Validation, Int. J. Multiphas. Flow 21 (1995) 351–363, https://doi.org/10.1016/0301-9322(94)00083-V.
[6] J.R. Fagundes Netto, J. Fabre, L. Peresson, Shape of long bubbles in horizontal slug flow, Int. J. Multiphas. Flow 25 (1999) 1129–1160, https://doi.org/10.1016/S0301-9322(99)00041-5.
[7] K.H. Bendiksen, D. Malnes, R. Moe, S. Nuland, The dynamic two-fluid model OLGA: theory and application, SPE Prod. Eng. 6 (1991) 171–180, https://doi.org/10.2118/19451-PA.
[8] T.K. Kyeldby, R.A.W.M. Henkes, O.J. Nydal, Lagrangian slug flow modeling and sensitivity on hydrodynamic slug initiation methods in a severe slugging case, Int. J. Multiphas. Flow 53 (2013) 29–39, https://doi.org/10.1016/j.ijmultiphaseflow.2013.01.002.
[9] R.I. Issa, M.H.W. Kempf, Simulation of slug flow in horizontal and nearly horizontal pipes with the two-fluid model, Int. J. Multiphas. Flow 29 (2003) 69–95, https://doi.org/10.1016/S0301-9322(02)00127-1.
[10] M. Bonizzi, P. Andreussi, S. Banerjee, Flow regime independent, high resolution multi-field modelling of near-horizontal gas-liquid flows in pipelines, Int. J. Multiphas. Flow 35 (2009) 34–46, https://doi.org/10.1016/j.ijmultiphaseflow.2008.09.001.
[11] M. Bonizzi, R.I. Issa, A model for simulating gas bubble entrainment in two-phase horizontal slug flow, Int. J. Multiphas. Flow 29 (2003) 1685–1717, https://doi.org/10.1016/j.ijmultiphaseflow.2003.09.001.
[12] A.J. Ortega Malca, A.O. Nieckele, Simulation of horizontal two-phase slug flow using the two-fluid model with a conservative and non-conservative formulation, in: Proceedings of the 8th International Congress of Mechanical Engineering, Ouro Preto, MG, 2005.
[13] A.V. Jones, A. Prosperetti, On the suitability of first-order differential models for two-phase flow prediction, Int. J. Multiphas. Flow 11 (1985) 133–148, https://doi.org/10.1016/0301-9322(85)90041-2.
[14] J.D. Ramshaw, A. Trapp, Characteristics, stability, and short-wavelength phenomena in two-phase flow equation systems, Nucl. Sci. Eng. 66 (1978) 93–102, https://doi.org/10.13182/NSE78-A15191.
[15] T.N. Dinh, R.R. Nourgaliev, T.G. Theofanous, Understanding the ill-posed two-fluid model, in: Proceedings of the 10th International Topical Meeting on Nuclear Reactor Thermal Hydraulics, NURETH10, Seoul, South Korea, 2003.
[16] A. Prosperetti, G. Tryggvason, Computational Methods for Multiphase Flow, Cambridge University Press, 2007.
[17] M.R. Baer, J.W. Nunziato, A two-phase mixture theory for the deflagration-to-detonation transition DDT in reactive granular materials, Int. J. Multiphas. Flow 12 (1986) 861–889, https://doi.org/10.1016/0301-9322(86)90033-9.
[18] R. Saurel, R. Abgrall, A multiphase Godunov method for compressible multifluid and multiphase flow, J. Comput. Phys. 150 (1999) 425–467, https://doi.org/10.1006/jcph.1999.6187.
[19] M.R. Ansari, A. Daramizadeh, Slug type hydrodynamic instability analysis using a five equations hyperbolic two-pressure, two-fluid model, Ocean Eng. 52 (2012) 1–12, https://doi.org/10.1016/j.oceaneng.2012.05.003.
[20] P. Loilier, C. Omgba-Essama, C. Thompson, Numerical experiments of two-phase flow in pipelines with a two-fluid compressible model, in: Proceedings of the 12th International Conference on Multiphase Production Technology, Barcellona, Spain, 2005. http://dspace.lib.cranfield.ac.uk/handle/1826/933.
[21] M. Ferrari, A. Bonzanini, P. Poesio, A 5-equation, transient, hyperbolic, 1-dimensional model for slug capturing in pipes, Int. J. Numer. Meth. Fluid. 85 (2017) 327–362, https://doi.org/10.1002/fld.4387.
[22] N. Brauner, D. Moalem Maron, Stability analysis of stratified liquid-liquid flow, Int. J. Multiphas. Flow 18 (1992) 103–121, https://doi.org/10.1016/0301-9322(92)90009-6.
[23] S.T. Munkejord, I.R. Gran, Modelling and Numerical Methods for Two-phase Flow, Volume PhD Thesis 2005, NTNU, VDM Verlag Dr. Muller Aktiengesell & Co. KG, Trondheim, Norway, 2009.
[24] D.J. Nicklin, Two phase bubble flow, Chem. Eng. Sci. 17 (1962) 693–702, https://doi.org/10.1016/0009-2509(62)85027-1.
[25] C. Foletti, S. Farisé, B. Grassi, D. Strazza, M. Lancini, P. Poesio, Experimental investigation on two-phase air/high-viscosity-oil flow in a horizontal pipe,

Chem. Eng. Sci. 66 (2011) 5968–5975, https://doi.org/10.1016/j.ces.2011.08.019.
[26] D. Picchi, Y. Manerba, S. Correra, M. Margarone, P. Poesio, Gas/shear-thinning liquid flows through pipes: modelling and experiments, Int. J. Multiphas. Flow 73 (2015) 217–226, https://doi.org/10.1016/j.ijmultiphaseflow.2015.03.005.
[27] D. Picchi, S. Correra, P. Poesio, Flow pattern transition, pressure gradient, hold-up predictions in gas/non-Newtonian power-law fluid stratified flow, Int. J. Multiphas. Flow 63 (2014) 105–115, https://doi.org/10.1016/j.ijmultiphaseflow.2014.03.005.
[28] N. Brauner, D. Moalem Maron, Analysis of stratified/nonstratified transitional boundaries in horizontal gas-liquid flows, Chem. Eng. Sci. 7 (1991) 1849–1859, https://doi.org/10.1016/0009-2509(91)87031-7.